Late Holocene earthquake history of the central Altyn Tagh fault, China

Zachary Washburn
J Ramón Arrowsmith
Department of Geological Sciences, Arizona State University, Tempe, Arizona 85287, USA
Steven L. Forman Department of Earth and Environmental Science, University of Illinois, Chicago, Illinois 60607, USA
Eric Cowgill Earth and Space Sciences Department, University of California, Los Angeles, California 90095-1567, USA
Wang Xiaofeng
Zhang Yueqiao
Chen Zhengle
Institute of Geomechanics, Beijing, China

ABSTRACT

The Altyn Tagh fault accommodates sinistral motion between the Tibetan Plateau and the Tarim block within the India-Eurasia collision zone. We used well-preserved evidence for surface-rupturing earthquakes to reconstruct the earthquake history for the central Altyn Tagh fault. We identified three geometric fault segments bounded by left steps and a bend. Geomorphic offsets indicate that the most recent event had maximum surface displacement of ~5.5 m in the west (38.5°N, 90.0°E), ~7 m in the central part of our study area, and ~4 m in the east (38.8°N, 91.5°E). The ^{14}C dates and trench logs of disrupted sediments indicate that these offsets occurred either in a single earthquake with a surface-rupture length >240 km dated as 680 ± 108 yr B.P. or as two events. If there were two events, the westernmost recent event occurred 518 ± 268 yr ago, whereas the eastern event occurred 650 ± 80 yr ago and had a surface rupture length >155 km. We find two events in the past 0.8–2.2 k.y. in the west and two or three events in the east, yielding recurrence intervals of 0.7 ± 0.4 k.y. and 1.1 ± 0.3 k.y., respectively. These recurrence rates for major earthquakes are lower than expected if the long-term fault slip rate is >20 mm/yr. Explanations for the discrepancy include an overdue major earthquake, or accelerated deformation elsewhere in the India-Eurasia orogen.

Keywords: Altyn Tagh fault, earthquake geology, India-Eurasia orogen, active tectonics.

INTRODUCTION

The sinistral Altyn Tagh fault traverses the northern boundary of Tibet for >1500 km and is a major structure in the India-Eurasia continental collision (Tapponnier and Molnar, 1977; Yin and Harrison, 2000). However, surprisingly little is published about its neotectonics and earthquake record. Study of the Altyn Tagh fault is important because it is one of the most prominent active strike-slip faults, and information about its earthquake behavior will contribute to our understanding of such structures; earthquake data about the fault will help clarify whether Asian continental deformation occurs along a handful of major faults separated by rigid blocks (e.g., Avouac and Tapponnier, 1993) or is distributed broadly among a few major faults and numerous smaller scale faults (e.g., England and Molnar, 1997). Global seismicity databases and the Chinese Catalog of Historic Strong Earthquakes (2300 B.C. to A.D. 1911) record no major events along the Altyn Tagh fault. However, we know that large earthquakes have occurred because of mole tracks seen on satellite imagery, surface breaks shown by Ge et al. (1992), and limited field investigation by western scientists (Molnar et al., 1987). In addition, recent work has focused on determining the slip rate by dating offset Quaternary landforms (Ryerson, 1997 [~25 mm/yr]; Meriaux et al., 2000 [3 cm/yr]) and global positioning system (GPS) measurements (Bendick et al., 2000; Shen et al., 2001 [~10 mm/yr]).

Another way to evaluate the activity of the Altyn Tagh fault is to study its earthquake history. To do this, we conducted a paleoseismic study that contributes quantitative earthquake frequency (recurrence intervals of 0.7 ± 0.4 and 1.1 ± 0.3 k.y.) and approximate magnitude data (M_w 7 to >7.8) for paleo-earthquakes along the Altyn Tagh fault. Detailed documentation of the active trace geometry and segment boundaries for a 150-km-long reach of the central fault serves as a framework for interpreting our paleoseismic data. Stratigraphic and structural relationships at three paleoseismic sites provide age information on recent earthquakes, and offset geomorphic features are used to infer peak displacement in the last earthquake.

OBSERVATIONS

Surface-Trace Geometry

In the field, we defined the active trace as the collection of fault traces that ruptured recently as indicated by the geomorphic age of the scarps. We used a 1 km left step and a 30° fault bend to separate the westernmost Wuzhunxiao segment from the central Pingding segment, which ends at a 4 km left step before the eastern Xorxoli segment begins (DePolo et al., 1991; Knuepfer, 1989; Fig. 1). In the next section we use the along-fault distance starting from the west to reference the location of important features.

Earthquake Geology of the Most Recent Earthquake

Historic and instrumental records show little seismicity (>M5) along the Altyn Tagh fault, but offset Holocene landforms and sharp mole tracks indicate that earthquakes have occurred recently. Displacement in those earthquakes can be determined from offset geomorphic features. The smallest offsets that span the fault zone and are not modified and the sharpest surface rupture should be the result of the most recent earthquake. Where we establish the most recent earthquake offset, larger offsets at the same site indicate slip from multiple events.

We measured the offset of abandoned gullies and narrow ridgelines in the field. The offset data have clearly interpretable restorations of landforms across a single fault strand. We evaluated the relative quality of each offset as an indicator of tectonic fault slip and estimated measurement uncertainty due to variation in projection and restoration of offset landform elements (Fig. 2A). We utilize offset distribution, geometric data, and surface-rupture morphology to estimate minimum surface-rupture length for the most recent earthquakes.

We recorded 7 offsets (~2–5 m) along the Wuzhunxiao segment, 3 (~3.5–5.5 m) along the Pingding segment, and 26 along the Xorxoli segment; the highest quality data are from km 97–136 (Figs. 1 and 2A). In the Gobiling basin (km 106–112), the arid climate and small catchments (<1 km^2) preserve remarkably crisp offset gullies (Fig. 1B). The modern gullies have the same morphology as the offset one and are a good analogy for the preoffset configuration of the displaced gullies. Five narrow gullies with intact debris-flow levees were offset between 6.1 ± 0.25 m and 7.4 ± 0.5 m during the most recent earthquake. The similar offset magnitude and continuous offset distribution along the entire Xorxoli segment indicate that the most recent earthquake here had peak displacement of

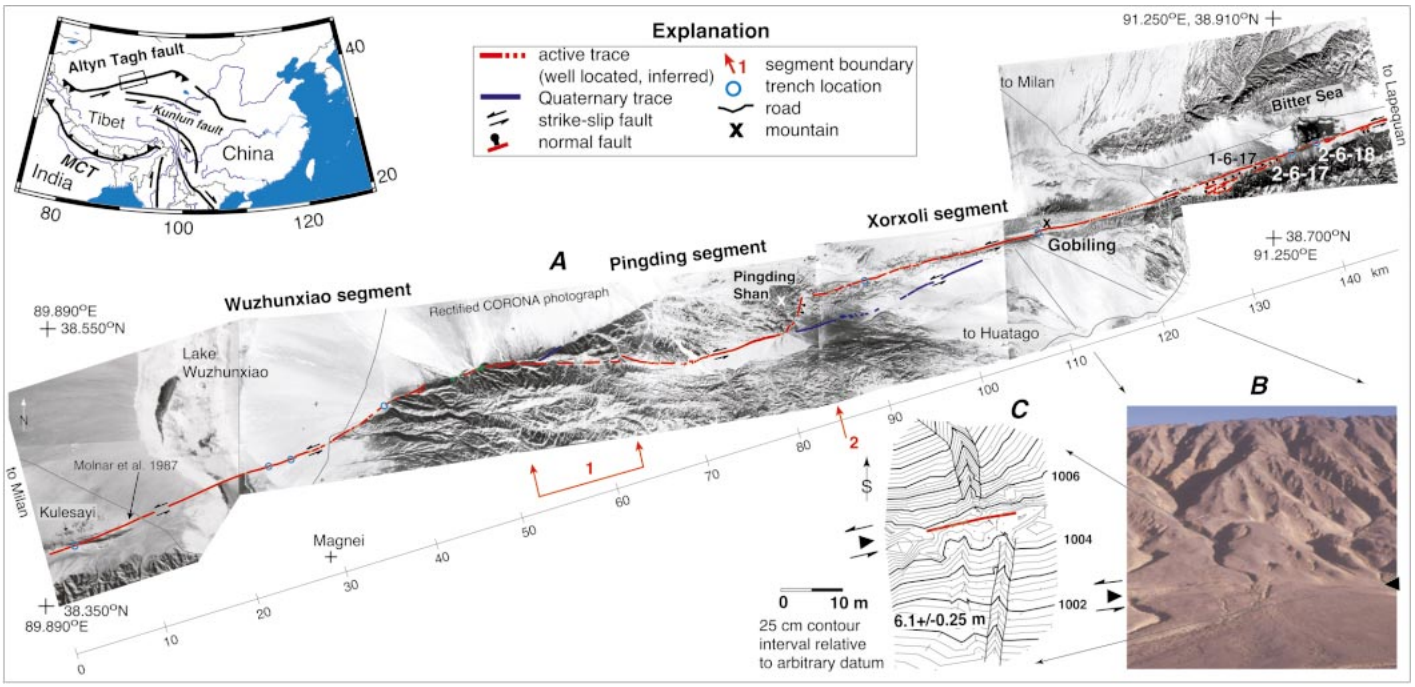

Figure 1. A: Map of active fault trace of central Altyn Tagh fault showing geometry of most recent and Quaternary rupture traces. Three geometric segments are defined and bounded by (1) 30° bend and 1 km left step and (2) 4 km left step. Scale below map and numbered locations correspond to descriptions in text. B: Photograph looking south at fault zone and 6.1 ± 0.25 m offset of incised gully at Gobiling recording maximum most recent earthquake displacement. Triangles mark fault trace. C: Contour map of this well-defined offset. MCT is Main Central thrust.

~7 m (km 97–136), which tapers to ~4 m at km 140 (Fig. 2A).

To determine the timing of past earthquakes, we made excavations across parts of the active trace where the steady accumulation of distinctive sediments would preserve evidence of past ruptures. In our paleoseismic trenches, upward terminations of fault traces and broken and tilted beds overlain by continuous beds identify past earthquakes. Disruption seen at the same stratigraphic level at several locations and on both trench walls qualifies as a distinct event. Organic matter within the stratigraphy was dated with ^{14}C, and fine silt was dated by infrared stimulated luminescence (IRSL).

An excavation of a small depression bounded by a shutter ridge shows evidence for the most recent earthquake at Kulesayi (km 3) (Figs. 1 and 3; also see Data Repository[1]). In the bottom of this trench, gravels buried a layer of vegetation on top of silt layers (shaded green) that were tilted by the penultimate event. Silt, fine sand, and some pebbly sand layers (shaded blue) were deposited conformably on those gravels, and the entire package was faulted. More fine sediments (shaded yellow) then buried the most recent earthquake fault scarps. Although it appears that two of the most recent faults cut the upper silt package, they are older because this is a buttress contact where sediments were deposited against an exposed scarp. A ^{14}C date from the vegetation layer (Beta-126349, A.D. 1215–1295 [calibrated years]) gives a maximum age

[1]GSA Data Repository item 2001122, Topographic map of Kulesayi site, geochronology tables for ^{14}C and IRSL samples, and topographic maps and trench logs of the 2-6-17 and 2-6-18 sites, is available from Documents Secretary, GSA, P.O. Box 9140, Boulder, CO 80301-9140, editing@geosociety.org, or at www.geosociety.org/pubs/ft2001.htm.

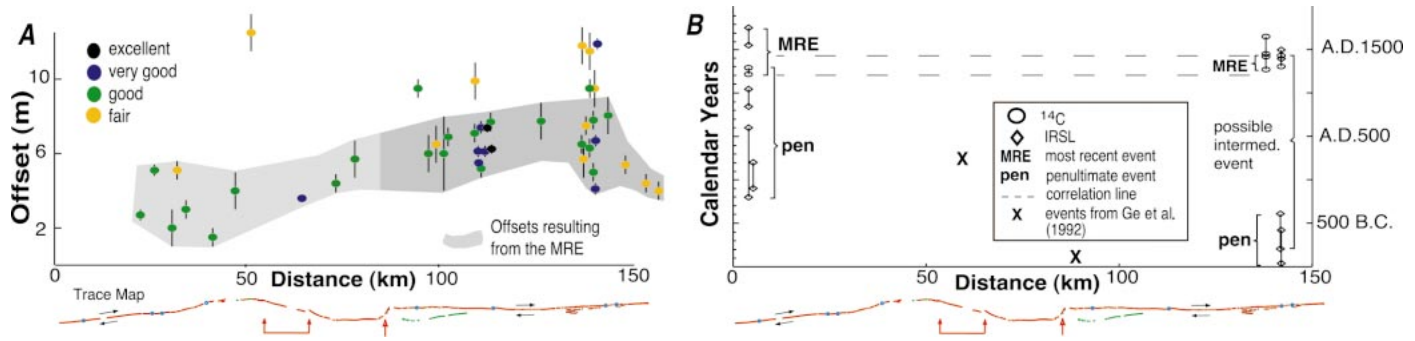

Figure 2. A: Offset geomorphic features vs. along-fault distance with active trace map below. Offsets ranging from 4 to 7 m cluster along Xorxoli segment, group of lower magnitude offsets are preserved along western segments, and third group of offsets ranging from 9 to 12 m is sporadically preserved. We interpret larger magnitude offsets to result from accumulated slip from more than one earthquake and 2–7 m offsets (gray shading) as displacement produced by most recent earthquake (MRE). B: Numerical age constraints for recent events on Altyn Tagh fault vs. along-fault distance. Infrared stimulated luminescence (IRSL) and ^{14}C dates from excavation at Kulesayi bracket MRE between A.D. 1215 and 1750 and penultimate event between A.D. 1050 and 200 B.C. IRSL and ^{14}C dates from excavations at 2-6-17 and 2-6-18 are combined to bracket Xorxoli MRE between A.D. 1270 and 1430, penultimate event between 400 B.C. and 1000 B.C., and possible intermediate event between 800 B.C. and A.D. 1430. Correlation lines show that it is possible that MRE ruptured all three segments between A.D. 1215 and 1430. However, two smaller earthquakes are more likely because Pingding left step probably barred rupture.

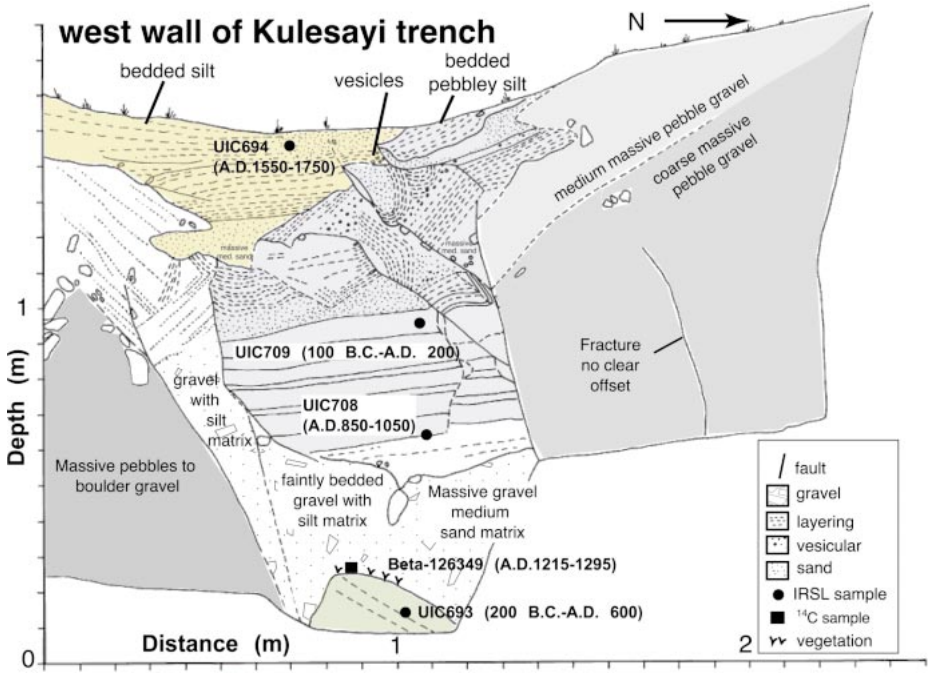

Figure 3. Trench log of Kulesayi site. See text for explanation. IRSL is infrared stimulated luminescence.

for the most recent earthquake, and overlying unfaulted silt deposits (UIC694, A.D. 1550–1750) provide a minimum age (Fig. 2B; Tables 1 and 2; see footnote 1). The stratigraphic relationships of UIC708 and UIC709 to Beta-126349 imply that these IRSL samples were probably not completely reset; thus we exclude them from further calculations.

Four paleoseismic excavations in the vicinity of the Bitter Sea define the timing on the Xorxoli segment (Fig. 1). The 2-6-17 site was surveyed to document the geometry of short normal faults that develop in an ~100 m left step (see footnote 1). An excavation across one of these normal faults revealed basal pebbly sand units forming a trough into which eolian sand was deposited. Dilation, resulting from the rupturing through the extensional left step, created a ≤20-cm-wide fissure into which blocks of the eolian sand, massive windblown silt, and salt grass leaves were deposited. This relationship of fissure fill of massive silts containing well-preserved salt grass leaves is also seen in three other trenches at this site. The ^{14}C dates from salt grass leaves (Beta-134382, A.D. 1270–1420) preserved in a unit cut by the fissure give a maximum age for the most recent earthquake, and ^{14}C dates from salt grass (Beta-134381) located at the top of the fissure provide a capping age of A.D. 1450–1650 (Fig. 2B). It is unlikely that the well-preserved leaves are much older than the deposit, because regular strong winds in this area contain wind-born sand that degrades these leaves quickly.

We excavated a 25-m-long trench on the lateral edge of a small alluvial fan where finely laminated silt, bedded sand, and gravel units are preserved (site 2-6-18, km 141; see footnote 1). Upward fault terminations in a gravel deposit overlying a sand package identify the most recent earthquake at this site (Fig. 4). These faults show predominantly strike-slip motion; however, a small component of dip slip forms a 30-cm-deep depression in the center of the trench. IRSL sample UIC724 taken from a faulted silt layer ~20 cm below the event horizon provides a maximum age of 800–400 B.C. The ^{14}C sample Beta-134384 from an overlying and unfaulted eolian unit deposited in the depression provides a capping age of A.D. 1305–1430. A similar date from a collocated IRSL sample (UIC723, A.D. 1400–1500) shows good agreement between these different dating methods (Fig. 2B).

Earthquake Geology of the Penultimate Rupture

The displacement produced by the penultimate Kulesayi event is unknown, and the maximum displacement of the penultimate Xorxoli event is uncertain because of the lack of a clear penultimate offset distribution. However, the 9–12 m offsets measured on the Xorxoli segment suggest that the penultimate event there had at least 5 m of slip (Fig. 2A). Evidence for this amount of slip is seen at site 1-6-17, where a channel is offset 10.9 ± 0.5 m. If this channel was offset ~7 m by the most recent earthquake, then the penultimate offset may be ~4 m at this site.

Although the record of slip in the penultimate event is poorly preserved, its age is indicated by

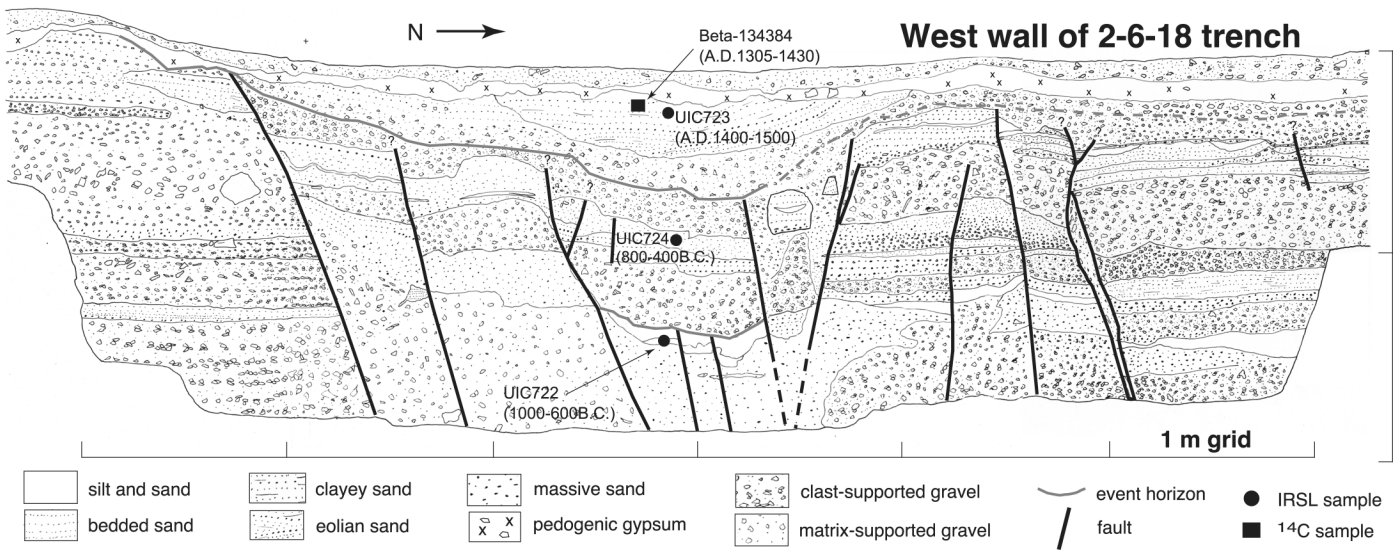

Figure 4. Trench log of 2-6-18 site. See text for explanation. IRSL is infrared stimulated luminescence.

stratigraphic relationships in our excavations. The discordance between the dips of the upper and lower silts as well as the buried vegetation define the penultimate event at Kulesayi (Fig. 3). The relationship of the silt and vegetation contact is uncertain; the vegetation may have been growing in the silt and therefore may have been killed by the penultimate event, or it may have fallen from above sometime after this event. The available evidence does not favor one scenario over the other; thus we can only say that the penultimate event occurred after deposition of the tilted silt package (UIC693, 200 B.C.–A.D. 600) and before death of the vegetation (A.D. 1215–1295) (Fig. 2B).

At site 2-6-18, the penultimate event is defined by upward fault terminations that cut a laminated silt and sand package, located ~40 cm from the base of the trench (Fig. 4). These faults offset only the silts and sands and do not rupture the overlying gravels. Sample UIC722 from the faulted silt provides a maximum date of 1000–600 B.C. for this event. UIC724 from a silt layer conformably overlying the unfaulted gravel provides a capping date of 800–400 B.C. for the penultimate event (Fig. 2B). There is a possible intermediate event, identified by two small faults in the middle of the trench that appear to terminate at the top of the sand package ~20 cm below the most recent earthquake event horizon. This event would have occurred sometime after the deposition of the upper sand package (800–400 B.C.).

DISCUSSION AND CONCLUSIONS

Mapping of latest Holocene rupture patterns characterizes active trace geometry, including one straight segment with associated normal faults, two bent segments, and two major geometric boundaries. The earthquake geology presented in this paper is not broad enough to determine the tectonic role of the Altyn Tagh fault in the continental collision, but it does provide an important quantification of its activity. To reconstruct the earthquake history, we synthesized all of the data presented in this paper and used regressions of surface-rupture length to estimate moment magnitude (M_w) for the most recent earthquake (Wells and Coppersmith, 1994). Excavations across the active traces and the lack of unconformities in these trenches provide an apparently complete earthquake record in the study area. We assumed that the Xorxoli most recent earthquake ruptured both sites 2-6-17 and 2-6-18 because they are only 3 km apart and the excavations across all prominent scarps at 2-6-17 diminished the potential for missing an event. Combining age data from both of these sites narrows the timing of the Xorxoli earthquake to between A.D. 1270 and 1430. The most recent Kulesayi earthquake occurred between A.D. 1215 and 1750; on the sole basis of timing, it is possible that one large event ruptured the entire field area between A.D. 1215 and 1430 (Fig. 2B). In this case, the earthquake would have jumped two geometric boundaries and ruptured from at least km 0 to km 147 and likely farther because of sharp surface rupture that continues to >km 240 (Washburn, 2001). This scenario yields a surface rupture length of >240 km and M_w of >7.8.

The different scarp morphology between the Xorxoli (sharp) and western segments (degraded) implies that these surface ruptures may not be the same age. In addition, it is likely that 4 km Pingding left step barred rupture because only 2 of 159 historical strike-slip surface ruptures have jumped extensional steps greater than 4 km (Knuepfer, 1989). If it did bar rupture, then the Xorxoli most recent earthquake had peak displacement of ~7 m and ruptured this entire segment and probably past km 240 (surface rupture length >155 km and M_w >7.6). The earthquake occurred between A.D. 1270 and 1430 because it ruptured through the Bitter Sea trenches. The Kulesayi most recent earthquake occurred between A.D. 1215 and 1750, but we cannot determine whether the surface rupture along the western segments was produced by one large or numerous smaller earthquakes because of similar scarp morphology and the lack of a clear offset distribution. If we speculate that the ~5.5 m offsets near km 20 were produced by the Kulesayi earthquake, then this offset would correspond to a low M_w 7 event.

Little is known about the penultimate Kulesayi event except that it occurred between 200 B.C. and A.D. 1295. The penultimate Xorxoli event had at least 5 m of slip and occurred between 400 and 1000 B.C. If the potential intermediate event seen at site 2-6-18 occurred, there would have been three Xorxoli earthquakes in the past 2.4–3.0 k.y.

To compare these paleo-earthquake data with other findings along the Altyn Tagh fault, we cast slip rate in terms of average recurrence intervals by using 5 and 10 m of slip per event, because these values bracket the peak offsets recorded for the most recent earthquakes. (1) Using ~10 mm/yr determined from GPS (Bendick et al., 2000; Shen et al., 2001) yields recurrence intervals of 0.5 and 1.0 k.y. for 5 and 10 m of slip per event, respectively. (2) Using ~3 cm/yr determined by large-scale postglacial offsets and offset terraces and moraines (Peltzer et al., 1989; Meriaux et al., 2000) yields recurrence times of 0.2 and 0.3 k.y. We find two to three earthquakes in the past 2.4–3.0 k.y. at the Bitter Sea and two Kulesayi events in the past 0.8–2.2 k.y. Although we have a limited number of events for robust recurrence calculations, taking averages from these data gives repeat times of 0.7 ± 0.4 k.y. for the Kulesayi site and 1.1 ± 0.3 k.y. for the Bitter Sea trenches. These frequencies are consistent with the two earthquakes in the past 3 k.y. in our study area reported by Ge et al. (1992) and are generally similar to the 800–1000 yr recurrence times estimated for the Kunlun fault (Van der Woerd et al., 1998).

Comparison of the different recurrence intervals shows that the earthquake data are consistent with the 10 mm/yr slip rate. One explanation for the discrepancy in average recurrence intervals is that a large earthquake is overdue. However, the long-term loading rate along the Altyn Tagh fault may have decreased since 100 ka and strain is now released elsewhere in Eurasia. However, if long recurrence intervals are representative of the neotectonic role of the Altyn Tagh fault in the India-Eurasia collision, then this result supports models with broader distribution of deformation rather than those with convergence accommodated along a few major faults bounding rigid blocks.

ACKNOWLEDGMENTS

We thank P. Molnar, R. Bilham, P. Tapponnier, M. Hamburger, R. Bürgmann, A. Yin, and J. Freymueller for useful reviews, our colleagues at the Institute of Geomechanics, and G. Sietz, S. Holloway, M. Baillie, S. Selkirk, E. Catlos, and S. Zhang. This work is part of a collaborative research effort supported by the U.S. National Science Foundation Continental Dynamics Program (grant EAR-9725780).

REFERENCES CITED

Avouac, P.J., and Tapponnier, P., 1993, Kinematic model of active deformation in central Asia: Geophysical Research Letters, v. 20, p. 895–898.

Bendick, R., Bilham, R., Freymueller, J., Larson, K., Peltzer, G., and Yin, G., 2000, Geodetic evidence for a low slip rate on the Altyn Tagh fault and constraints on the deformation of Asia: Nature, v. 404, p. 69–72.

DePolo, C.M., Clark, D., Slemmons, B., and Ramelli, A., 1991, Historical surface faulting in the western Basin and Range Province, western North America: Implications for fault segmentation: Journal of Structural Geology, v. 13, p. 122–136.

England, P.C., and Molnar, P., 1997, The field of crustal velocity in Asia calculated from Quaternary rates of slip on faults: Geophysical Journal International, v. 130, p. 551.

Ge, S., and 34 others, 1992, Active Altun fault zone monograph: State Seismological Bureau of China, p. 1–319.

Knuepfer, P.L.K., 1989, Implications of the characteristics of end-points of historical surface fault ruptures for the nature of fault segmentation, *in* Schwartz, D., and Sibson, R., eds., Fault segmentation and controls of rupture initiation and termination: U.S. Geological Survey Open-File Report 89-315, p. 193–228.

Meriaux, A.S., Ryerson, F.J., Tapponnier, P., Van der Woerd, J., Finkel, R., et al., 2000, Fast extrusion of the Tibet Plateau: A 3cm/yr, 100 kyr slip-rate on the Altyn Tagh fault: Eos (Transactions, American Geophysical Union), v. 81, p. 1137.

Molnar, P., Burchfiel, C., K'uangyi, L., and Ziyun, Z., 1987, Geomorphic evidence for active faulting in the Altyn Tagh and northern Tibet and qualitative estimates of its contribution to the convergence of India and Eurasia: Geology, v. 15, p. 249–253.

Peltzer, G., Tapponnier, P., and Armijo, R., 1989, Magnitude of late Quaternary left-lateral displacements along the north edge of Tibet: Science, v. 246, p. 1285–1289.

Ryerson, F.J., 1991, Rapid slip on the Altyn Tagh fault–Karakax valley segment: Geological Society of America Abstracts with Programs, v. 29, no. 6, p. A143.

Shen, Z.K., Wang, M., Li, Y., Jackson, D., Yin, A., Dong, D., and Fang, P., 2001, Crustal deformation along the Altyn Tagh fault system, western China, from GPS: Journal of Geophysical Research (in press).

Tapponnier, P., and Molnar, P., 1977, Active faulting and tectonics in China: Journal of Geophysical Research, v. 82, p. 2905–2930.

Van der Woerd, J., Ryerson, F.J., Tapponnier, P., Gaudemer, Y., and Finkel, R., 1998, Holocene left-slip rate determined by cosmogenic surface dating on the Xidatan segment of the Kunlun fault (Qinghai, China): Geology, v. 26, p. 695–698.

Washburn, Z., 2001, Quaternary tectonics and earthquake geology of the central Altyn Tagh fault, Xinjiang, China: Implications for tectonic process along the northern margin of Tibet [M.S. thesis]: Tempe, Arizona State University, 179 p.

Wells, D.L., and Coppersmith, K., 1994, New empirical relationships among magnitude, rupture length, rupture width, rupture area, and surface displacement: Seismological Society of America Bulletin, v. 84, p. 974–1002.

Yin, A., and Harrison, M., 2000, Geologic evolution of the Himalayan-Tibetan orogen: Annual Review of Earth and Planetary Sciences, v. 28, p. 211–280.

Manuscript received March 26, 2001
Revised manuscript received June 29, 2001
Manuscript accepted July 11, 2001

Printed in USA